JPE 19-6-23

https://doi.org/10.6113/JPE.2019.19.6.1575
ISSN(Print): 1598-2092 / ISSN(Online): 2093-4718

Improved Reactive Power Sharing and Harmonic Voltage Compensation in Islanded Microgrids Using Resistive-Capacitive Virtual Impedance

Minh-Duc Pham* and Hong-Hee Lee†

†,*School of Electrical Engineering, University of Ulsan, Ulsan, Korea

Abstract

Due to the mismatched line impedance among distributed generation units (DGs) and uncontrolled harmonic current, the droop controller has a number of problems such as inaccurate reactive power sharing and voltage distortion at the point of common coupling (PCC). To solve these problems, this paper proposes a resistive-capacitive virtual impedance control method. The proposed control method modifies the DG output impedance at the fundamental and harmonic frequencies to compensate the mismatched line impedance among DGs and to regulate the harmonic current. Finally, reactive power sharing is accurately achieved, and the PCC voltage distortion is compensated. In addition, adaptively controlling the virtual impedance guarantees compensation performance in spite of load changes. The effectiveness of the proposed control method was verified by experimental results.

Key words: Inaccurate reactive power sharing, Islanded microgrid, PCC voltage distortion, Virtual impedance

I. INTRODUCTION

Distributed generation (DG) has increased in power systems as a potential solution to meet the increased demand for electricity, reduce stress on transmission systems, and incorporate renewable energy resources. Subsequently, the microgrid concept has become a promising approach to coordinate different types of distributed energy resources [1]. Fig. 1 shows the basic structure of a microgrid with DGs connected in parallel, which is able to operate in both grid-connected and islanded modes. In the islanded mode, a droop controller is normally used so that the DGs can maintain a constant voltage at the point of common coupling (PCC) bus and autonomously share the load power [2].

Active power is proportionally shared among DGs with a droop controller, but reactive power sharing is inaccurate due to mismatched line impedances among DGs [3]. To eliminate the influence of line impedance mismatch, a modified Q-V droop controller and a power transformation were proposed to decouple the reactive power and the mismatched line impedance [4], [5]. However, the reactive power sharing error was only mitigated, and prior knowledge of system parameters is required. To eliminate parameter dependence, a small real power disturbance was injected into a microgrid to compensate for the reactive power sharing error [6]. However, the injected power disturbance reduces the accuracy of the DG output frequency and decreases microgrid stability. Accurate reactive power sharing and a precise DG frequency were realized by adding a large virtual inductance at the DG inverter output [7], [8]. However, this strategy affects the voltage control precision and reduces the microgrid voltage quality. An adaptive virtual impedance control method was presented to improves voltage quality, but the system dynamic performance was not good due to power coupling [9].

In addition to the reactive power sharing issue, voltage harmonic distortion at the PCC is also a big concern since the droop controller only regulates fundamental components. When a nonlinear load is connected to the grid, the uncontrolled harmonic currents result in instability in the microgrid and PCC voltage distortion. A harmonic droop controller was presented to regulate voltage harmonics at the PCC [10], [11]. However, the additional harmonic droop control loop reduces the dynamic performance of the active and reactive power

Manuscript received Jul. 25, 2019; accepted Aug. 26, 2019
Recommended for publication by Associate Editor Sung-Jin Choi.
†Corresponding Author: hhee@mail.ulsan.ac.kr
Tel: +82-52-259-2187, Fax: +82-52-259-1686, University of Ulsan
*School of Electrical Engineering, University of Ulsan, Korea

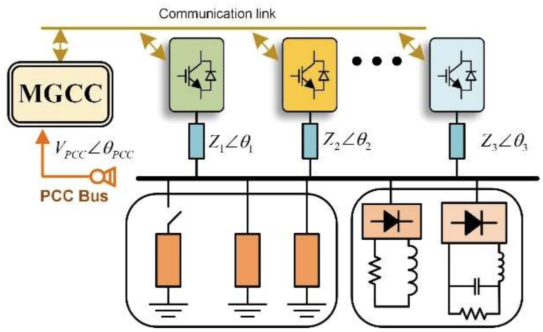

Fig. 1. Typical islanded microgrid configuration.

sharing. To eliminate this problem, either a virtual harmonic resistance [12] or a virtual capacitance [13] can be added to the DG output impedance to regulate harmonic currents. However, these methods have limited compensating performance in case of a long transmission line and increased system disturbances, which reduce the stability and reliability of microgrids. On the other hand, a virtual harmonic inductance was introduced to regulate the DG output impedance at the harmonic frequency for absorbing nonlinear load current [14]. Although the PCC voltage quality was improved, the large virtual inductance reduced system stability. The virtual harmonic impedance was optimized based on a state-space model of a microgrid, but the feasibility of this method is limited since exact system parameters are required [15].

To overcome these existing limitations, this paper proposes a resistive-capacitive (RC) virtual impedance control method for reactive power sharing accuracy and PCC harmonic voltage compensation. To achieve these control objectives, an RC virtual fundamental impedance is added at the output of a DG inverter to compensate mismatched line impedance. As a result, the reactive power sharing error is eliminated. In addition, an RC virtual harmonic impedance is proposed to modify the DG output impedance at the harmonic frequency for harmonic current compensation. The effectiveness of the proposed control method was verified by experimental results.

II. Conventional Droop Control Algorithm

A. Basic Principle of a Droop Control Algorithm

To realize power sharing and to synchronize each DG, the traditional $P-\omega$ and $Q-V$ droop controllers are adopted. Their equations are given in (1) and (2), respectively:

$$\omega_i = \omega_0 - G_{Pi} P_i, \tag{1}$$

$$V_i = V_0 - G_{Qi} Q_i, \tag{2}$$

where the index i represents each DG, ω_i and ω_0 are the output and nominal values of the DG output frequency, V_i and V_0 are the output and nominal values of the DG output voltage, G_{Pi} and G_{Qi} are the active and reactive droop coefficients, and P_i and Q_i are the output active and reactive powers, respectively. Fig. 2 shows the characteristics of the $P-\omega$ and $Q-V$ droop controllers. From Fig. 2, it can be seen that the DG output frequency and voltage magnitude are regulated according to the output active and reactive powers. Hence, all of the DGs with the droop controller can autonomously share the total load power in an islanded microgrid.

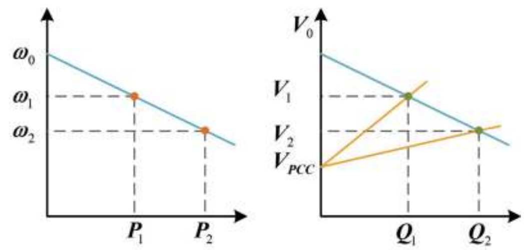

Fig. 2. $P-\omega$ and $Q-V$ droop control characteristics.

From the droop controller, the DG output voltage reference is defined as follows:

$$V_{dri} = V_i \sin\left(\int \omega_i \, dt\right) \quad . \tag{3}$$

In (3), the voltage reference of the droop controller only consists of fundamental components. Therefore, when a nonlinear load is connected to the grid, the uncontrolled harmonic currents distort the PCC voltage and reduce system stability.

B. Reactive Power Sharing Issue

In a DG transmission system, the line impedance is mainly inductive because of the LCL filter inductance, and the output reactive power of the i[th] DG (i=1,2) is approximated as follows [16]:

$$Q_i \cong \frac{V_{PCC}\left(V_i - V_{PCC}\right)}{X_{\ln i}} \quad , \tag{4}$$

where $X_{\ln i}$ is the line reactance of the i[th] DG. By substituting (2) into (4), the reactive power sharing error (ΔQ) is obtained as follows:

$$\begin{aligned}\Delta Q &= G_{Q1}Q_1 - G_{Q2}Q_2 \\ &= \frac{V_{PCC}\left(V_0 - V_{PCC}\right)\left(G_{Q1}X_{\ln 2} - G_{Q2}X_{\ln 1}\right)}{\left(G_{Q1}V_{PCC} + X_{\ln 1}\right)\left(G_{Q2}V_{PCC} + X_{\ln 2}\right)}.\end{aligned} \tag{5}$$

It is assumed that the two DGs have the same rated power $\left(G_{Q1} = G_{Q2}\right)$ for the sake of a simple analysis. Thus, ΔQ in (5) becomes zero only when $\left(G_{Q1}X_{\ln 2} - G_{Q2}X_{\ln 1}\right) = 0$. However, the line inductance among the DGs is not the same ($X_{\ln 1} \neq X_{\ln 2}$) due to different DG locations. Therefore, the reactive power sharing error ΔQ in (5) is inevitable. Furthermore, since the parasitic line resistance is neglected in (5), the reactive power sharing accuracy cannot be guaranteed in practical applications. Therefore, it is necessary to compensate the

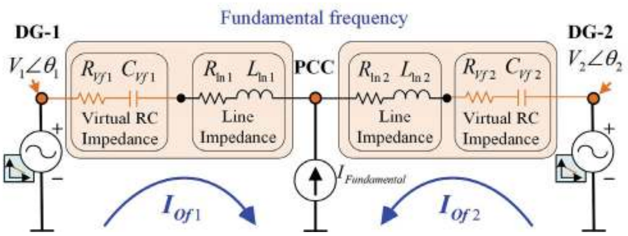

Fig. 3. Equivalent circuit of 2 DGs for the fundamental frequency.

mismatched line impedance to achieve accurate reactive power sharing.

III. Proposed Control Strategy

A. Resistive-Capacitive Virtual Impedance

In order to compensate the mismatched line impedance, a virtual capacitance is proposed to counteract the effect of the physical line inductance in (5). In addition, a virtual resistance is also considered to compensate for the effect of the parasitic line resistance. The equivalent circuit of two paralleled DGs for the fundamental frequency is shown in Fig. 3. The proposed virtual resistor (R_{Vfi}) and capacitor (C_{Vfi}) of the i[th] DG in Fig. 3 are regulated by using the following external control loops:

$$R_{Vf\,i}=\left(K_{iP}/s\right)\left(P_i^*-P_i\right), \tag{6}$$

$$C_{Vf\,i}=\left(K_{iQ}/s\right)\left(Q_i^*-Q_i\right), \tag{7}$$

where P_i^* and Q_i^* are the reference active and reactive powers, which are calculated by the microgrid central controller (MGCC):

$$P_i^*=\left(1/\mathrm{G}_{Pi}\right)\left(1/\left(\sum_{i=1}^{n}1/\mathrm{G}_{Pi}\right)\right)\sum_{i=1}^{n}P_i\,, \tag{8}$$

$$Q_i^*=\left(1/\mathrm{G}_{Qi}\right)\left(1/\left(\sum_{i=1}^{n}1/\mathrm{G}_{Qi}\right)\right)\sum_{i=1}^{n}Q_i\,, \tag{9}$$

where n is the total number of DGs in the microgrid. The RC virtual impedance at the fundamental frequency $Z_{Vf\,i}$ is obtained as follows:

$$Z_{Vf\,i}=R_{Vf\,i}+\frac{1}{sC_{Vf\,i}}\,. \tag{10}$$

Bode diagrams of $Z_{Vf\,i}$ with a number of specific values are shown in Fig. 4. From Fig. 4, it is obvious that the RC virtual impedance in (10) combines all of the characteristics of the resistance and capacitance. When compared to the conventional methods [7], [8], which only regulate the magnitude of the virtual impedance, the proposed control method can flexibly control both the phase and magnitude of the virtual impedance. Thus, the proposed RC virtual impedance overcomes the phase difference issue in the conventional method, and the line impedance mismatch among DGs is effectively compensated.

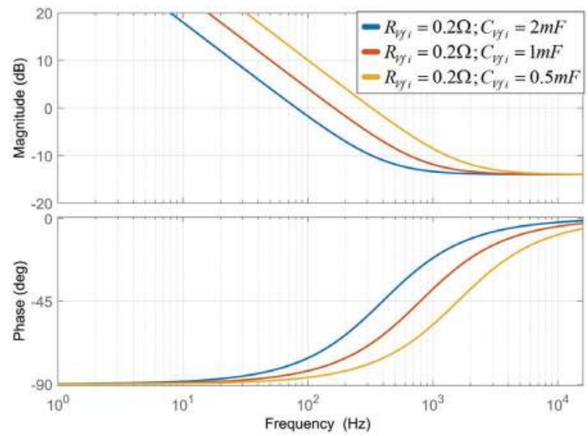

Fig. 4. Bode diagrams of the RC fundamental virtual impedance.

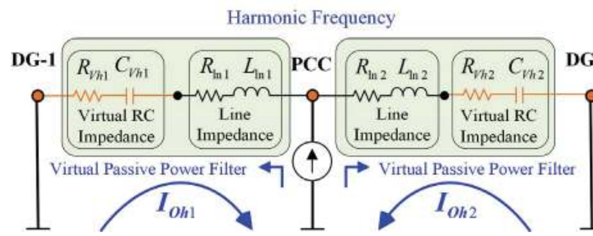

Fig. 5. Equivalent circuit of 2 DGs for the harmonic frequency.

B. Harmonic Voltage Compensation

In order to compensate the PCC harmonic voltage, the proposed resistive-capacitive virtual impedance can be extended for the harmonic frequency to regulate the harmonic current. Fig. 5 shows an equivalent circuit of a microgrid for the harmonic frequency. From Fig. 5, the proposed RC virtual impedance is coordinated with the line inductance to form a virtual passive filter. By controlling the RC virtual impedance, the passive filter resonance is adaptively regulated to meet the PCC harmonic frequency, and the PCC voltage distortion is compensated.

To show the effectiveness of the proposed RC virtual impedance, Bode diagrams of the DG equivalent impedance at the 3[rd] harmonic frequency are plotted in Fig. 6. The DG equivalent impedance at the 3[rd] harmonic frequency is reduced significantly thanks to the RC virtual impedance. Therefore, the DG absorbs more of the load harmonic current, and the 3[rd] PCC harmonic voltage is compensated.

In the ideal case, the virtual harmonic resistance (R_{Vhi}) is set as zero to compensate the PCC voltage with a high performance. However, the ideal value of $R_{Vh\,i}$ reduces the system stability due to the increased sensitivity to PCC voltage harmonics variation [17]. Therefore, the value of $R_{Vh\,i}$ should be large enough to enhance the system damping and small enough to maintain the harmonic compensating performance.

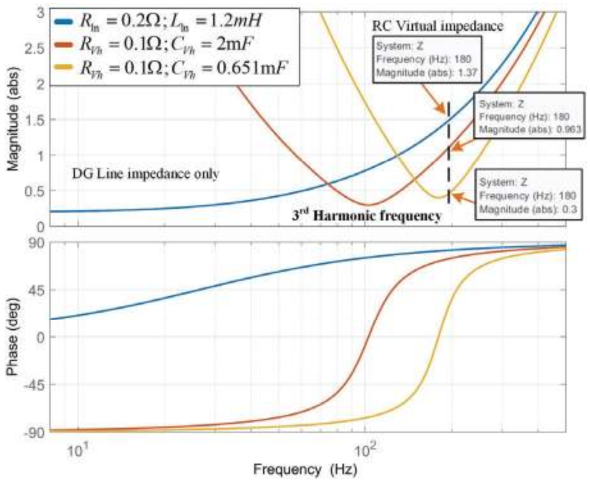

Fig. 6. Block diagrams of the DG equivalent impedance at the 3rd harmonic frequency with the RC virtual impedance.

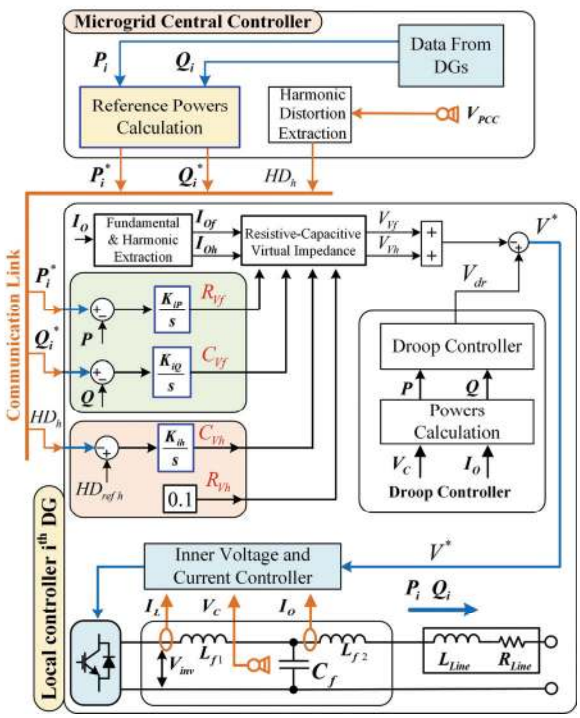

Fig. 7. Block diagram of the proposed control method.

To satisfy these constraints, the virtual harmonic resistance is chosen from 0.1Ω to 3Ω [17], [18]. In this paper, the virtual harmonic resistance (R_{Vhi}) is set as 0.1Ω, while the virtual harmonic capacitance (C_{Vhi}) is adjusted continuously:

$$C_{Vhi} = \left(K_{ih}/s\right)\left(HD_{ref\,h} - HD_h\right), \tag{11}$$

where $HD_{ref\,h}$ and HD_h are the reference and present values of the h[th] PCC harmonic distortion, and HD_h is given as:

$$HD_h = \left(\frac{V_{PCC}^h}{V_{PCC}^f}\right)100\%, \tag{12}$$

where V_{PCC}^h and V_{PCC}^f are the RMS values of the PCC

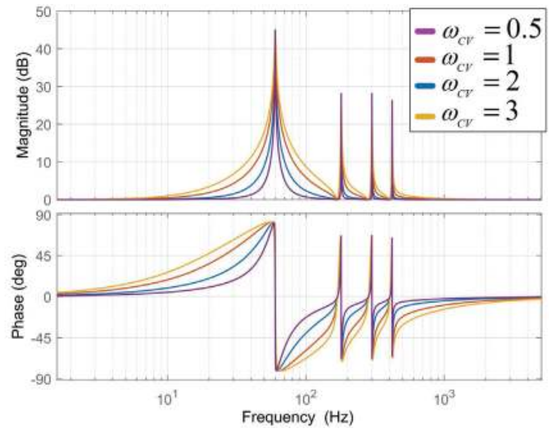

Fig. 8. Bode diagrams of multi non-ideal PR controllers.

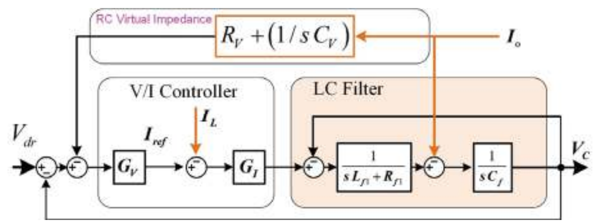

Fig. 9. Block diagram of the inner voltage and current control loops.

harmonic and fundamental voltages, respectively. To reduce the DG computation burden, the MGCC measures and extracts the PCC harmonic components. These values are sent to all of the DGs in the microgrid. A block diagram of the proposed control method is shown in Fig. 7.

C. Inner Voltage and Current Controllers

In order to effectively track the voltage reference, the following multiple non-ideal proportional-resonant (PR) voltage and current controllers are applied to regulate the DG output voltage:

$$G_V(s) = K_{PV} + \sum_{h=1,3,5,7} \frac{2K_{IVh}\,\omega_{CV}\,s}{s^2 + 2\omega_{CV}\,s + \omega_h^2}\ , \tag{13}$$

$$G_I(s) = K_{PI}\ , \tag{14}$$

where K_{PV} and K_{PI} are the proportional gains, K_{IVh} is the resonant gain of the PR controller, and ω_{CV} and ω_h are the cut-off frequency and resonance frequency of the PR controller, respectively.

Fig. 8 shows Bode diagrams of the non-ideal PR controller with different values of ω_{CV}. From Fig. 8, it is obvious that the PR controller has a high gain at both the fundamental and harmonic frequencies for enforcing a small steady-state error. Since a disturbance always exists in islanded microgrids, the PR controller bandwidth needs to be optimized to ensure system stability. For this purpose, ω_{CV} is chosen as 1 rad/s to minimize the system disturbance and the steady-state error. A block diagram of the inner voltage and current control loops is shown in Fig. 9.

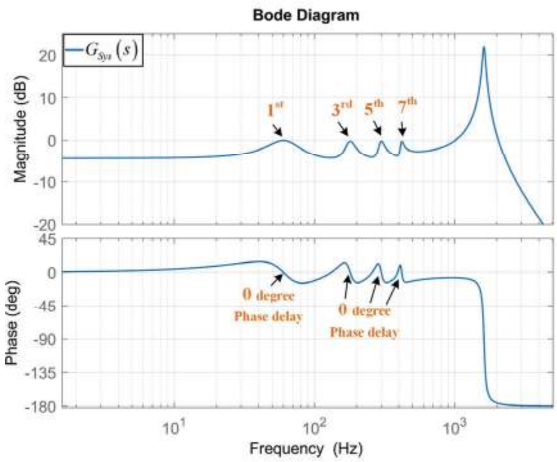

Fig. 10. Bode diagrams of the DG voltage gain $G_{sys}(s)$.

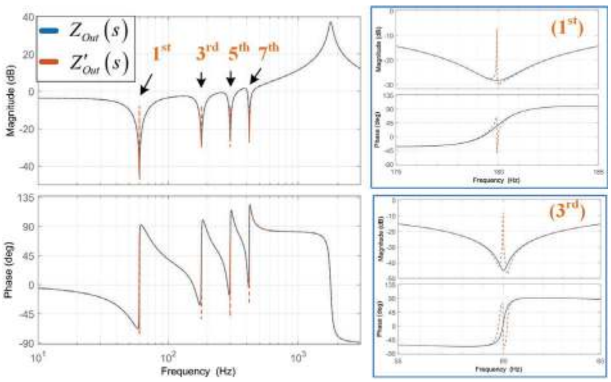

Fig. 11. Bode diagrams of the DG output impedance $Z_{Out}(s)$ and $Z'_{Out}(s)$.

D. Output Impedance Analysis

The closed-loop transfer function of the system without considering the virtual impedance is obtained from Fig. 9:

$$V_C = G_{sys}(s)V^* - Z_{Out}(s)I_O . \tag{15}$$

In (15), $G_{sys}(s)$ and $Z_{Out}(s)$ are the transfer functions of the DG voltage gain and the output impedance, respectively, which are given below:

$$G_{sys}(s) = \frac{G_V G_I}{s^2 L_f C_f + sR_f C_f + sG_I C_f + G_V G_I + 1}, \tag{16}$$

$$Z_{Out}(s) = \frac{(sL_f + R_f + G_I)}{s^2 L_f C_f + sR_f C_f + sG_I C_f + G_V G_I + 1}. \tag{17}$$

By considering the proposed RC virtual impedance, the DG output impedance $Z_{Out}(s)$ is modified as follows:

$$Z'_{Out}(s) = Z_{Out}(s) + G_{Sys}(s)\, Z_V(s) . \tag{18}$$

To evaluate the effectiveness of the proposed controller, the frequency-amplitude characteristic of the DG voltage gain $G_{sys}(s)$ is plotted in Fig. 10. From Fig. 10, the magnitudes of $G_{sys}(s)$ are equal to 1 for all of the 1st, 3rd, 5th and 7th frequencies.

TABLE I
SYSTEM PARAMETERS

Parameters	Values	Parameters	Values
K_{iP}	$0.5e^{-2}$	L_{f1}	1.2mH
K_{iQ}	$5e^{-2}$	R_{f1}	0.02Ω
K_{ih}	$1e^{-3}$	L_O	1.2mH
K_{PI}	2	C_f	20uF
K_{PV}	1.0	G_{Pi}	0.012
K_{IVh}	20	G_{Qi}	0.015
Z_{ln1}	0.1+0.39j Ω	V_0	110V
Z_{ln2}	0.15+0.7j Ω	ω_0	377 rad/s
Z_{ln3}	0.2+1.1j Ω	ω_{CV}	1 rad/s
Load Change	10Ω 45mH	$HD_{ref\,3,5,7}$	1%

In addition, the voltage drop between the voltage reference and the DG output voltage becomes zero. Furthermore, the phase of $G_{sys}(s)$ at both the fundamental and harmonic frequencies is close to 0, which shows that the output voltage has zero phase delay. Thus, it can be said that the inner controllers perfectly track the voltage reference.

Fig. 11 shows Bode diagrams of the DG output impedances $Z_{Out}(s)$ and $Z'_{Out}(s)$. From Fig. 11, it is clear that the modified output impedance $Z'_{Out}(s)$ has a sufficient gain at both the fundamental and harmonic frequencies to compensate the mismatched line impedance as well as the PCC voltage harmonics. As a result, reactive power sharing is accurately achieved, and the system dynamic performance is guaranteed even if the load changes. In addition, the PCC voltage harmonics are effectively compensated by means of the RC virtual impedance.

IV. EXPERIMENTAL RESULTS

The effectiveness of the proposed control method is experimentally verified with 3 DGs in Fig. 1, and the experimental parameters are given in Table I. The DGs are controlled using a Texas Instruments DSP TMS320F28379D microcontroller, and the laboratory islanded microgrid system with 3 DGs is shown in Fig. 12.

Fig. 13 shows the power sharing performance of the microgrid with the proposed controller. From Fig. 13, the active power is shared equally among the DGs with the conventional droop controller. However, the reactive power is not accurately shared due to the mismatched line impedance. When the proposed controller is applied, the RC virtual impedance is inserted to compensate the unequal line impedance. As a result, the reactive power sharing is accurately achieved after a short transient period as shown in Fig. 13. In addition, accurate active power sharing is still guaranteed during reactive power compensation with a small transient oscillation

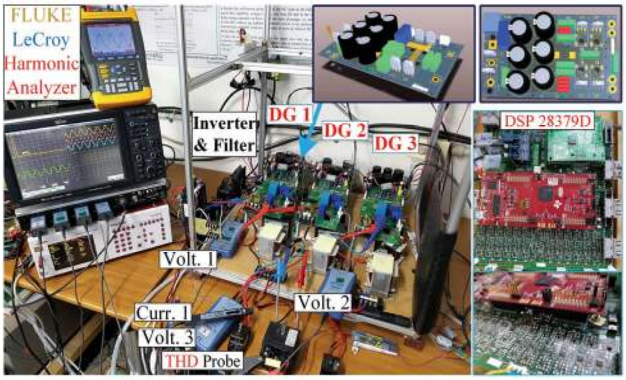

Fig. 12. Laboratory islanded microgrid system.

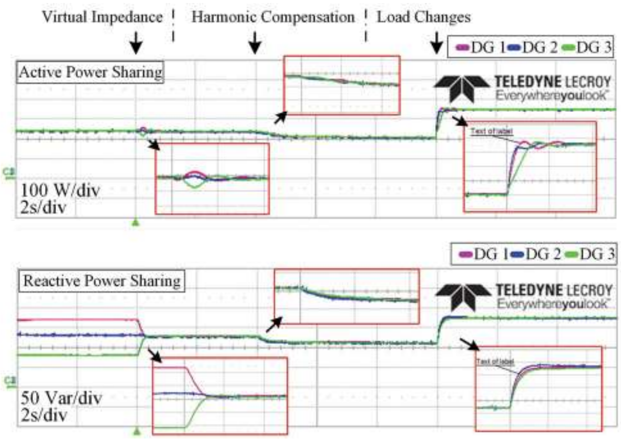

Fig. 13. Power sharing performance with the proposed controller.

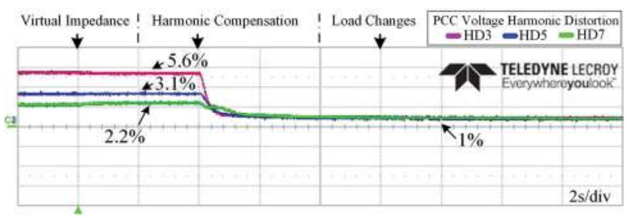

Fig. 14. Performance of the PCC harmonic voltage compensation.

by means of the proposed virtual resistance. Furthermore, the RC virtual impedance is continuously tuned to keep accurate power sharing even though harmonic compensation and load power changes, as can be seen in Fig. 13.

Fig. 14 shows the performance of the PCC harmonic voltage compensation. From Fig. 14, HD_3, HD_5 and HD_7 are initially 5.6%, 3.1% and 2.2%, respectively. It can also be seen they are all reduced to 1% with a smooth response after compensation. In spite of load changes, the harmonic compensation shows good dynamic performance. In order to investigate the transient performance of the proposed controller, the PCC voltage is measured and shown in Fig. 15. In Fig. 15, the PCC voltage harmonics are seamlessly compensated without any oscillations or fluctuations, and the desired harmonic distortions are accurately achieved. From these experimental

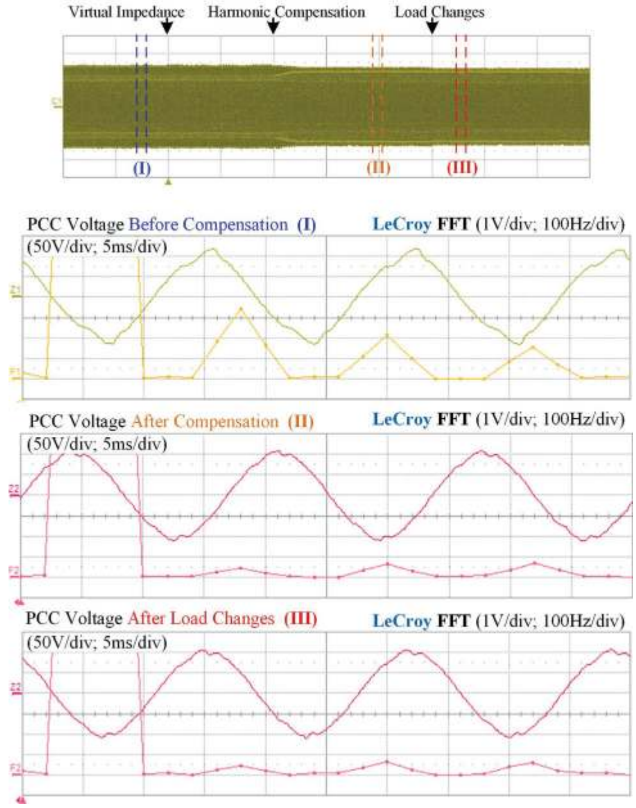

Fig. 15. PCC harmonic voltage quality with the proposed controller.

results, it can be seen that the proposed RC virtual impedance method shows a good performance with a fast and smooth response.

V. Conclusions

This paper has eliminated the reactive power sharing error by proposing the use of RC virtual fundamental impedance to compensate the mismatched line impedance This study proposed RC virtual fundamental impedance to compensate for mismatched line impedance to eliminate the reactive power sharing error. In addition, the desired PCC harmonic compensation is accurately achieved by considering the RC virtual impedance at harmonic frequencies. The RC virtual impedance is regulated by an external control loop in a DG. In addition, its impedance values are adaptively tuned to ensure accurate reactive power sharing in spite of the load power changes. A number of experimental results show the effectiveness and feasibility of the proposed control method.

Acknowledgment

This work was supported by the National Research Foundation of Korea Grant funded by the Korean Government (NRF-2018R1D1A1A09081779).

REFERENCES

[1] D. E. Olivares, A. Mehrizi-Sani, A. H. Etemadi, C. A. Cañizares, R. Iravani, M. Kazerani, A. H. Hajimiragha, O. Gomis-Bellmunt, M. Saeedifard, R. Palma-Behnke, G. A. Jiménez-Estévez, and N. D. Hatziargyriou, "Trends in microgrid control," *IEEE Trans. Smart Grid*, Vol. 5, No. 4, pp. 1905-1919, Jul. 2014.

[2] Y. W. Li and C. N. Kao, "An accurate power control strategy for power-electronics-interfaced distributed generation units operating in a low-voltage multibus microgrid," *IEEE Trans. Power Electron.*, Vol. 24, No. 12, pp. 2977-2988, Dec. 2009.

[3] H. Han, X. Hou, J. Yang, J. Wu, M. Su, and J. M. Guerrero, "Review of power sharing control strategies for islanding operation of AC microgrids," *IEEE Trans. Smart Grid*, Vol. 7, No. 1, pp. 200-215, Jan. 2016.

[4] K. De Brabandere, B. Bolsens, J. Van den Keybus, A. Woyte, J. Driesen, and R. Belmans, "A Voltage and Frequency Droop Control Method for Parallel Inverters," *IEEE Trans. Power Electron.*, Vol. 22, No. 4, pp. 1107-1115, Jul. 2007.

[5] C. T. Lee, C. C. Chu, and P. T. Cheng, "A new droop control method for the autonomous operation of distributed energy resource interface converters," *IEEE Trans. Power Electron.*, Vol. 28, No. 4, pp. 1980-1993, Apr. 2013.

[6] J. He, Y. W. Li, and F. Blaabjerg, "An enhanced islanding microgrid reactive power, imbalance power, and harmonic power sharing scheme," *IEEE Trans. Power Electron.*, Vol. 30, No. 6, pp. 3389-3401, Jun. 2015.

[7] X. Wang, Y. W. Li, F. Blaabjerg, and P. C. Loh, "Virtual-impedance-based control for voltage-source and current-source converters," *IEEE Trans. Power Electron.*, Vol. 30, No. 12, pp. 7019-7037, Dec. 2015.

[8] J. Liu, Y. Miura, H. Bevrani, and T. Ise, "Enhanced virtual synchronous generator control for parallel inverters in microgrids," *IEEE Trans. Smart Grid*, Vol. 8, No. 5, pp. 2268-2277, Sep. 2017.

[9] H. Mahmood, D. Michaelson, and J. Jiang, "Accurate reactive power sharing in an islanded microgrid using adaptive virtual impedances," *IEEE Trans. Power Electron.*, Vol. 30, No. 3, pp. 1605-1617, Mar. 2015.

[10] T.-L. Lee and P.-T. Cheng, "Design of a new cooperative harmonic filtering strategy for distributed generation interface converters in an islanding network," *IEEE Trans. Power Electron.*, Vol. 22, No. 5, pp. 1919-1927, Sep. 2007.

[11] M. Savaghebi, A. Jalilian, J. C. Vasquez, and J. M. Guerrero, "Selective compensation of voltage harmonics in an islanded microgrid," in *2nd Power Electronics, Drive Systems and Technologies Conference*, pp. 279-285, 2011.

[12] P. Sreekumar and V. Khadkikar, "A new virtual harmonic impedance scheme for harmonic power sharing in an islanded microgrid," *IEEE Trans. Power Del.*, Vol. 31, No. 3, pp. 936-945, Jun. 2016.

[13] Q. C. Zhong and Y. Zeng, "Control of inverters via a virtual capacitor to achieve capacitive output impedance," *IEEE Trans. Power Electron.*, Vol. 29, No. 10, pp. 5568-5578, Oct. 2014.

[14] B. Liu, Z. Liu, J. Liu, R. An, H. Zheng, and Y. Shi, "An adaptive virtual impedance control scheme based on small-AC-signal injection for unbalanced and harmonic power sharing in islanded microgrids," *IEEE Trans. Power Electron.*, Vol. 34, No. 12, pp. 12333-12355, Mar. 2019.

[15] J. Roldan-Perez, A. Rodriguez-Cabero, and M. Prodanovic, "Harmonic virtual impedance design for parallel-connected grid-tied synchronverters," *IEEE J. Emerg. Sel. Top. Power Electron.*, Vol. 7, No. 1, pp. 493-503, Mar. 2019.

[16] Y. Han, H. Li, P. Shen, E. A. A. Coelho, and J. M. Guerrero, "Review of active and reactive power sharing strategies in hierarchical controlled microgrids," *IEEE Trans. Power Electron.*, Vol. 32, No. 3, pp. 2427-2451, Mar. 2017.

[17] H. Fujita and H. Akagi, "A practical approach to harmonic compensation in power systems series connection of passive and active filters," *IEEE Trans. Ind. Appl.*, Vol. 27, No. 6, pp. 1020-1025, Nov. 1991.

[18] W. Wu, Y. Sun, M. Huang, X. Wang, H. Wang, F. Blaabjerg, M. Liserre, and H. S. H. Chung, "A robust passive damping method for LLCL-filter-based grid-tied inverters to minimize the effect of grid harmonic voltages," *IEEE Trans. Power Electron.*, Vol. 29, No. 7, pp. 3279-3289, Jul. 2014.

Minh-Duc Pham was born in Lam Dong, Vietnam, in 1992. He obtained his B.S. degree in Electrical Engineering from the Ho Chi Minh City University of Technology and Education, Ho Chi Minh City, Vietnam, in 2014. Since 2015, he has been working towards his M.S./Ph.D. degrees in the School of Electrical Engineering, University of Ulsan, Ulsan, Korea. He worked for one year as an R&D Engineer at the SolarBK Co., Ho Chi Minh City, Vietnam, where he was conducting research on photovoltaic cells and designing system controllers. His current research interests include harmonic control technologies, renewable energy sources and hybrid AC/DC microgrid systems.

Hong-Hee Lee received his B.S., M.S. and Ph.D. degrees in Electrical Engineering from Seoul National University, Seoul, Korea, in 1980, 1982 and 1990, respectively. From 1994 to 1995, he was a Visiting Professor at the Texas A&M University, College Station, TX, USA. Since 1985, he has been with the Department of Electrical Engineering, University of Ulsan, Ulsan, South Korea, where he is currently a Professor in the School of Electrical Engineering. He was also the Director of the Network-based Automation Research Center (NARC), which was sponsored by the Ministry of Trade, Industry and Energy. His research interests include power electronics, network-based motor control, and renewable energy. Dr. Lee is a member of the Institute of Electrical and Electronics Engineers (IEEE), the Korean Institute of Power Electronics (KIPE), the Korean Institute of Electrical Engineers (KIEE), and the Institute of Control, Robotics and Systems (ICROS). He was the President of KIPE in 2014.